Wildy, P., & Watson, D. H. (1962) *Cold Spring Harbor Symp. Quant. Biol. 27*, 25-47.
Williams, R. C. (1977) *Proc. Natl. Acad. Sci. U.S.A. 74*, 2311-2315.
Wimmer, E. (1982) *Cell (Cambridge, Mass.) 28*, 199-201.
Wold, F. (1981) *Annu. Rev. Biochem. 50*, 783-814.
Yamamoto, K. R., & Alberts, B. M. (1970) *Virology 40*, 734-744.

X-ray Crystallographic and Nuclear Magnetic Resonance Spectral Studies of the Products from the Yeast Inorganic Pyrophosphatase-$Co(NH_3)_4PP$ Reaction. Investigation of the Pyrophosphatase Reaction Mechanism†

Tuli P. Haromy, Wilson B. Knight, Debra Dunaway-Mariano,* and M. Sundaralingam*

ABSTRACT: Yeast inorganic pyrophosphatase catalyzes the hydrolysis of P^1,P^2-bidentate $Co(NH_3)_4$ pyrophosphate [$Co(NH_3)_4PP$] to the cis, bis(phosphate) complex $Co(NH_3)_4(P_i)_2$, which is not stable at neutral pH and over a period of 24 h converts to HPO_4^{2-} and a mixture of bidentate $Co(NH_3)_4(PO_4)$ and monodentate $Co(NH_3)_4(H_2O)(HPO_4)$. Concurrent with this process is the reduction and subsequent release of $Co(H_2O)_6^{2+}$ from the cobalt tetraammine bis(phosphate) complex and/or the cobalt tetraammine monophosphate complex. Bidentate tetraammine phosphatocobalt(III), hexaaquocobalt(II), orthophosphate, and two free water molecules cocrystallize [$Co(NH_3)_4PO_4 \cdot Co(H_2O)_6^{2+} \cdot HPO_4^{2-} \cdot 2H_2O$] from the reaction mixture in the triclinic space group $P\bar{1}$ ($Z = 2$) with cell dimensions $a = 6.849$ (1) Å, $b = 11.693$ (2) Å, $c = 12.630$ (2) Å, $\alpha = 65.60$ (1)°, $\beta = 88.98$ (1)°, and $\gamma = 73.04$ (1)°. The structure was solved by the heavy atom technique and refined to an R index of 0.040 by using 3077 intensities measured up to a 2θ limit of 155°. ^{31}P NMR studies of the equilibrium mixture reveal that the equilibrium constant is a sensitive function of solution pH and temperature. Unlike the $Co(NH_3)_4PP$ complex, there is evidence indicating that the $Mg(H_2O)_4PP$ complex is degraded to monodentate $Mg(H_2O)_5PO_4$ in the enzyme active site.

Yeast inorganic pyrophosphatase catalyzes the hydrolysis of inorganic pyrophosphate. The enzyme requires a minimum of two divalent cations per subunit for activity (Knight et al., 1981; Springs et al., 1981; Cooperman et al., 1981; Rapoport et al., 1973). Several models for metal-pyrophosphate or metal-phosphate interactions during catalysis have been presented (Knight et al., 1981; Konsowitz & Cooperman, 1976; Avaeva et al., 1977; Rapoport et al., 1973; Springs et al., 1981; Sperow & Butler, 1976). The results from studies in our laboratory are most consistent with a mechanism in which water coordinated to a second enzyme-bound metal ion adds to the phosphorus atom of the P^1,P^2-bidentate metal-pyrophosphate complex resulting in the cleavage of the phosphoanhydride linkage and formation of *cis*-metal$(H_2O)_4(P_i)_2$. This complex may then be released directly from the enzyme or undergo further hydrolysis (of the M-O-P bond) prior to release. Magnesium, which serves as the metal cofactor in vivo, forms kinetically unstable complexes with polyphosphates, making isolation and structural characterization of the pyrophosphatase substrate, intermediate, and product metal complexes impractical. However, if Co(III)-complexed pyrophosphate is used as the substrate, the product complex should be of sufficient stability to permit structural studies to be carried out. This study was undertaken to determine the structures and stability of the reaction products resulting from the pyrophosphatase-catalyzed hydrolysis of $Co(NH_3)_4PP$.

Materials and Methods

Preparation and Structure Analysis of Tetraammine(phosphato)cobalt(III) Hexaaquocobalt(II) Hydrogen Phosphate (2-) Dihydrate Crystals. A 3-mL solution 10 mM in $Co(NH_3)_4PP$ (Cornelius et al., 1977), 50 mM in Pipes [piperazine-*N*,*N*′-bis(2-ethanesulfonic acid)] (K^+ salt, pH 7.5), 1 mM in Mg^{2+}, and 300 units/mL in pyrophosphatase was allowed to proceed to equilibrium at 25 °C. After 24 h, most of the reaction product had crystallized. X-ray diffractometer intensity data were collected on these crystals (observed density = 2.02 g/cm^3, calculated density = 2.010 g/cm^3) using Ni-filtered Cu Kα radiation ($\lambda = 1.5418$ Å). Out of a total of 3703 unique reflections measured up to a 2θ limit of 155°, 3077 reflections with $I/\sigma(I)$ greater than 1.5 were used for the structure analysis. The data were corrected for crystal decay (approximately 4%), Lorentz, and polarization effects. The data were also corrected for X-ray absorption ($\mu = 15.0$ mm^{-1}) by using a two-parameter empirical absorption correction based on both ϕ and θ with a maximum ϕ correction of 33% at $\theta = 13°$ and 14% at $\theta = 64°$.

A Patterson synthesis showed a very strong vector at $x, y, z = (^1/_2, 0, ^1/_2)$, consistent with an intensity distribution: strong for $h + l$ even and weak for $h + l$ odd. This indicates the presence of a cobalt atom at (0, 0, 0) and ($^1/_2$, 0, $^1/_2$) or alternatively at ($^1/_4$, 0, $^1/_4$) and ($^3/_4$, 0, $^3/_4$). The former possibility would be inconsistent with the cis, bis complex $Co(NH_3)_4(P_i)_2$, which was believed to be the crystalline py-

† From the Department of Biochemistry, College of Agricultural and Life Sciences, University of Wisconsin—Madison, Madison, Wisconsin 53706 (T.P.H. and M.S.), and the Department of Chemistry, University of Maryland, College Park, Maryland 20742 (W.B.K. and D.D.-M.).
Received July 22, 1982. This work was supported in part by National Institutes of Health Grant GM-17378 to M.S. and by National Institutes of Health Grant GM-28688 to D.D.-M. D.D.-M. received a research career development award from the National Institutes of Health (ES-00111). Acknowledgment is made to the donors of the Petroleum Research Fund, administered by the Americal Chemical Society, for partial support of this research.

0006-2960/82/0421-6950$01.25/0

rophosphatase reaction product (Knight et al., 1981), since it does not have a center of inversion. Consequently, the initial attempt at solving the structure was centered around placing the cobalt atom at ($^1/_4$, 0, $^1/_4$). Since this approach failed to yield a solution, the presence of the cis complex was questioned and further work was performed by assuming the cobalt atoms to be on the inversion centers. Inclusion of two additional atoms found from the Patterson map [which turned out to be a third cobalt atom and the associated phosphorus atom of the tetraammine(phosphato)cobalt complex] together with the special position cobalt atoms provided sufficient phasing information to solve the structure.

The heavy-atom parameters were refined to convergence using first isotropic and then anisotropic temperature factors (see paragraph at end of paper regarding supplementary material). All of the hydrogen atoms were subsequently located on difference Fourier syntheses. The structure was further refined by the full matrix least-squares technique with unit weights using anisotropic temperature factors for the nonhydrogen atoms and isotropic temperature factors for the hydrogen atoms to a final R index of 0.040. The average and maximum shift/error ratios after refinement were 0.02 and 0.12 for nonhydrogen and hydrogen atoms, respectively.

The scattering factors for the nonhydrogen atoms were taken from Cromer & Waber (1965), those for hydrogen atoms were from Stewart et al. (1965), and the anomalous corrections to the nonhydrogen scattering factors were from the *International Tables for X-ray Crystallography* (1974).

^{31}P NMR Studies of the Pyrophosphatase Reaction. ^{31}P NMR spectra were recorded at 23 °C using a Varian XL-100 NMR spectrometer (40.5 mHz). All chemical shifts are reported as ppm relative to a 0.1 M D_3PO_4 external standard. The pyrophosphatase reaction was examined under conditions which led to immediate turnover of the $Co(NH_3)_4PP$ (a) and conditions which allowed examination of the reaction at varying conversions (b). (a) A 2-mL, 55% D_2O solution 114 μM in pyrophosphatase active sites, 23 mM in $Co(NH_3)_4PP$, 18 mM in Mg^{2+}, 0.5 mM in EDTA, and 80 mM in Pipes (K^+ salt, pH 6.7) was incubated at 23 °C for 30 min and analyzed (30-min data acquisition period). The ^{31}P NMR spectrum was measured again after 2 h had elapsed from the initiation of the reaction (1-h data acquisition time). (b) A 5-mL, 50% D_2O solution 4 μM in pyrophosphatase active sites, 60 mM in $Co(NH_3)_4PP$, 20 mM in Mg^{2+}, 4 mM in EDTA, and 100 mM in Pipes (K^+ salt, pH 6.7) was incubated at 23 °C. The ^{31}P spectrum of the reaction mixture was analyzed after 3 h and again after 17 h.

^{31}P Studies of the $Co(NH_3)_4PO_4$ to $Co(NH_3)_4(H_2O)PO_4$ Equilibrium. The reaction product crystals were dissolved at a concentration of 20 mg/mL in 30 mM HCl in D_2O. The solution was made 15 mM in EDTA and adjusted to the desired pH by using KOH. Equilibrium conditions were ensured by determining the monodentate to bidentate ratio of freshly prepared solutions and of solutions that were allowed to equilibrate for 12 h. In addition, we found that the same equilibrium position was reached regardless of whether the sample at a given pH was prepared by raising the pH of an equilibrated sample or by decreasing it. The $Co(NH_3)_4PO_4$ (5 mM) solutions used for the temperature studies were first treated with Chelex to remove Co(II) and then made 1 mM in EDTA and 40 mM in phosphate buffer at pH 6.7.

Radioisotopic Assay of the $Co(NH_3)_4PP$ Hydrolysis Reaction. A solution 0.77 mM in $Co(NH_3)_4PP$ (2×10^{10} cpm/mmol), 20 mM in $MgCl_2$, 60 mM in Pipes (K^+ salt, pH 7.0), and 0.02 mM in pyrophosphatase active sites was incubated at 27 °C for 50 min. So that the $Co(NH_3)_4(P_i)_2$ complex could be separated from the enzyme, half of the solution was passed down a Sephadex G-25 column (1.2 × 50 cm) equilibrated with 20 mM $MgCl_2$ in 60 mM Pipes (pH 7). At various time intervals aliquots were taken from each of the two $Co(NH_3)_4(P_i)_2$ samples and loaded on a 1 mL Dowex 50-X2 (H^+) column. The column was washed with 7 mL of H_2O, followed by 7 mL of 2.5 M HCl. The amount of $[^{32}P]P_i$ in the acid and water wash was determined by liquid scintillation counting. From a plot of percent counts in H_2O wash vs. time, the rate of P_i release from the $Co(NH_3)_4(P_i)_2$ complex in the presence of pyrophosphatase was determined to be 0.077%/min while the rate of P_i release in the absence of pyrophosphatase was determined to be 0.073%/min.

Results

Crystal Structure of Tetraammine(phosphato)cobalt(III) Hexaaquocobalt(II) Hydrogen Phosphate (2–) Dihydrate. The final positional parameters are given in Table I. An ORTEP (Johnson, 1976) drawing of the crystalline reaction product including the tetraammine(phosphato)cobalt(III) complex is shown in Figure 1 with all nonhydrogen bond lengths and the chelate ring bond angles indicated. In the (phosphato)cobalt complex, two oxygen atoms of the phosphate group are chelated to the metal with ammines filling the remaining four coordination sites. Neither of the free phosphate oxygens is protonated, thus giving the phosphate a charge of 3–, balancing the cobalt charge of 3+. The structure contains a free orthophosphate molecule which is monoprotonated and thus has a 2– charge. This negative charge (two HPO_4^{2-} in the unit cell) balances the 2+ charges on the hexaaquocobalt groups. The unit cell also contains four free water molecules of crystallization (two in each asymmetric unit).

The four-membered ring of the (phosphato)cobalt complex is rather strained and thus significantly perturbs the ring angles from their ideal values. The O1(P1)–Co(1)–O2(P1) angle of the (phosphato)cobalt complex is contracted to 76.1° from the preferred octahedral angle of 90°. Similarly, the O1(P1)–P(1)–O2(P1) angle of 98.0° is also considerably less than the tetrahedral angle of 109.47°. The bond angles at O1(P1) and O2(P1), both equal to 92.9°, are also significantly contracted to permit formation of the four-membered ring. The chelate ring is nearly planar with the greatest deviation from the best least-squares plane through the four atoms being 0.026 Å for the phosphorus atom. The Co–NH_3 coordination distances range from 1.938 to 1.959 Å, which agree well with those previously reported for similar cobalt complexes (Merritt & Sundaralingam, 1980), while the hexaaquocobalt(II) groups at the inversion centers have Co–H_2O coordination distances ranging from 2.036 to 2.158 Å.

The bond lengths and angles can be compared to the corresponding values for the crystal structure of (phosphato)bis(ethylenediamine)cobalt(III) (Anderson et al., 1977) which contains two molecules in the asymmetric unit. The greatest difference for bond lengths and angles of the chelate ring between the two structures is 0.012 Å and 0.7°, respectively. One of the two independent molecules in the asymmetric unit has a planar chelate ring (maximum deviation from the plane = 0.02 Å) while the other molecule is slightly puckered (maximum deviation from the plane = 0.024 Å). The cobalt to phosphorus distance in the present structure is 2.563 Å compared to an average of 2.554 Å for the two molecules in the previous structure.

Figure 2 shows the various components of the crystalline reaction product with all hydrogen-bonding contacts indicated. A list of all the hydrogen-bonding interactions in the crystal

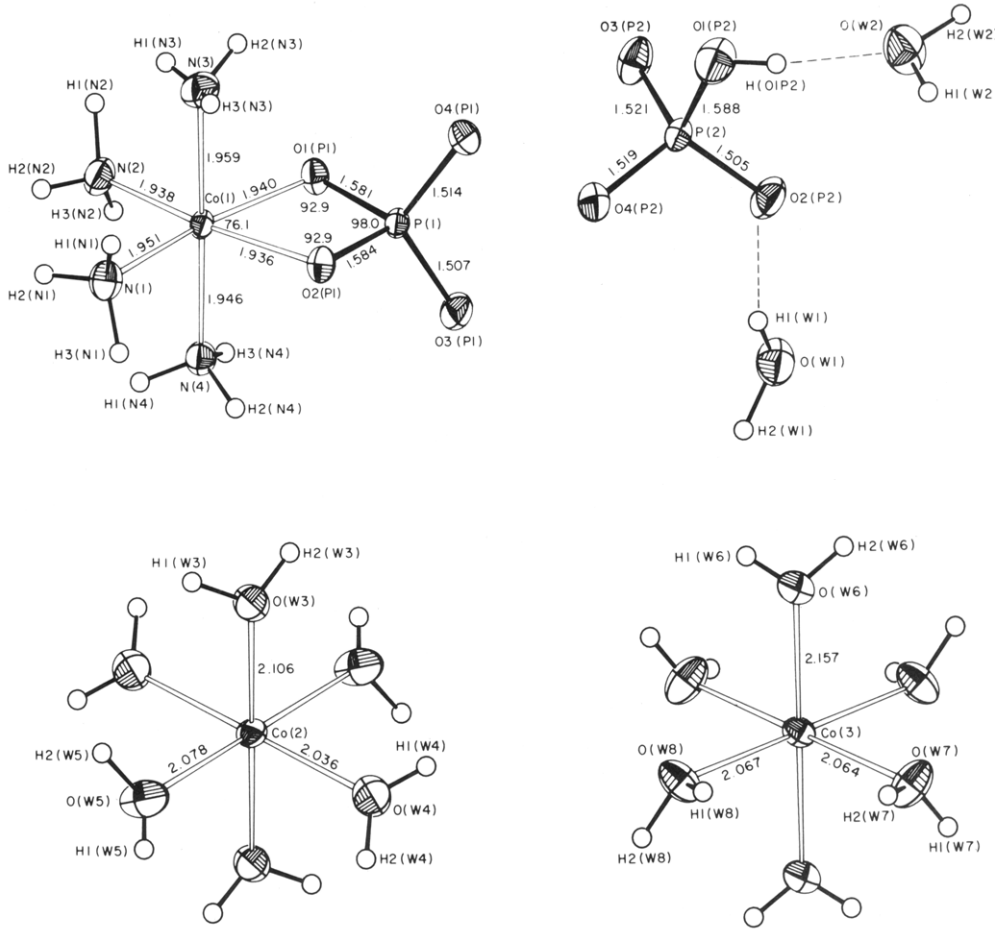

FIGURE 1: An ORTEP drawing showing the components of the crystalline reaction product. Nonhydrogen atoms are shown as 50% thermal probability ellipsoids and hydrogen atoms are shown as spheres of arbitrary size.

structure is given in Table II. Every proton in the crystal structure except for H1(N3) is engaged in hydrogen bonding with hydrogen-bond distances ranging from 2.622 to 3.135 Å. Virtually all of the strong hydrogen bonds involve the phosphate oxygens. The average N–H···O hydrogen bond distance of 3.02 (7) Å is approximately 0.3 Å longer than the average O–H···O hydrogen-bond distance of 2.73 (7) Å. The angles at the hydrogen-bonded protons range from 149° to 177° except for the weak N(3) to O(W7) hydrogen bond which has an angle of 132°.

^{31}P NMR and Radioisotopic Studies of the $Co(NH_3)_4PP$ Pyrophosphatase Reaction. The ^{31}P NMR spectrum of the $Co(NH_3)_4PP$ (60 mM)–pyrophosphatase (4 μM) reaction mixture was recorded after a reaction period of 3 h and again after 17 h. The first spectrum was characterized by a singlet at 11 ppm assigned to *cis*-$Co(NH_3)_4(P_i)_2$ and by a singlet at 4.2 ppm assigned to $Co(NH_3)_4PP$. From the integrals of the signals, it was determined that 19% of the $Co(NH_3)_4PP$ had been hydrolyzed. Prior to recording the 17-h spectrum, crystals which had formed in the reaction solution were removed by filtration. The NMR spectrum of the supernatant was characterized by singlets assigned to $Co(NH_3)_4(P_i)_2$ (11 ppm), $Co(NH_3)_4PP$ (4.2 ppm), $Co(NH_3)_4PO_4$ (24 ppm), and P_i (2.1 ppm). The relative ratios of these species were determined to be 9:1:1:1, respectively. Owing to the broadness of the $Co(NH_3)_4(PO_4)$ resonance, the relative concentration of the complex remaining in the supernatant could only be approximated.

The $Co(NH_3)_4PP$ (23 mM)–pyrophosphatase (114 μM) reaction, which reaches equilibrium in 10 min, yielded a spectrum after 30 min characterized by two singlets in an 8.7:1 ratio arising from $Co(NH_3)_4(P_i)_2$ and $Co(NH_3)_4PP$, respectively. The spectrum measured after a 3-h reaction period was not significantly different from the 30-min spectrum.

The possibility of pyrophosphatase-catalyzed P_i released from $Co(NH_3)_4(P_i)_2$ was carefully checked by measuring the rate of P_i loss from $Co(NH_3)_4(P_i)_2$ in the presence and absence of enzyme. At pH 7, 27 °C, the rates were essentially identical. P_i release from $Co(NH_3)_4(P_i)_2$ appeared to level off at 50% loss which suggests that P_i loss from $Co(NH_3)_4(P_i)$ is relatively slow. We have, in fact, found using ^{31}P NMR techniques that solutions of $Co(NH_3)_4(P_i)$ at or near neutral pH are stable to P_i loss for at least a period of 15 h.

^{31}P NMR Studies of $Co(NH_3)_4(PO_4)$. An attempt to elucidate the source of the $Co(H_2O)_6^{2+}$ formed in the $Co(NH_3)_4PP$–pyrophosphatase reaction mixture was made by examining the rate at which $Co(NH_3)_4PP$ releases pyrophosphate at pH 7.1 (25 °C). After a 24-h incubation period at pH 7.1 (25 °C), 20% of the substrate complex, as judged by the ^{31}P NMR spectrum of the mixture, had been converted to pyrophosphate. We judge that the mechanism of the pyrophosphate release involves reduction of the Co(III) complexes by Co^{2+} which is a persistent trace contaminant of our $Co(NH_3)_4PP$ preparation. The reduction process is very slow in acidic solutions in which the substrate complex is stored; however, it becomes significant at and above pH 7. Presumably, the Co^{2+} formed in the pyrophosphatase reaction is derived from the $Co(NH_3)_4(P_i)_2$ and/or $Co(NH_3)_4(PO_4)$ complexes and once formed it cocrystallizes with $Co(NH_3)_4(PO_4)$ and P_i (Scheme I).

The ^{31}P NMR spectra of solutions prepared from the crystals described above are characterized by a broad singlet

Table I: Fractional Positional Parameters for All Atoms of the Crystalline Reaction Product[a]

atom	x	y	z	B_{eq}[c] or B (Å²)
Co(1)	2151 (1)	5714 (1)	6376 (1)	1.05 (1)
P(1)	1410 (1)	7220 (1)	4175 (1)	1.13 (2)
O1(P1)	−55 (4)	6656 (2)	5093 (2)	1.49 (6)
O2(P1)	3442 (4)	6634 (2)	5054 (2)	1.44 (6)
O3(P1)	1667 (5)	6660 (2)	3281 (2)	2.03 (7)
O4(P1)	717 (4)	8715 (2)	3642 (2)	1.73 (7)
N(1)	4656 (5)	4902 (3)	7471 (3)	1.87 (8)
N(2)	442 (5)	4909 (3)	7503 (3)	1.86 (8)
N(3)	1447 (6)	7243 (3)	6750 (3)	2.12 (9)
N(4)	2876 (5)	4174 (3)	6035 (3)	1.55 (8)
P(2)	3516 (2)	2864 (1)	959 (1)	1.36 (2)
O1(P2)	2984 (5)	4135 (3)	1214 (2)	2.72 (8)
O2(P2)	3271 (5)	3296 (3)	−344 (2)	2.38 (8)
O3P(2)	2033 (5)	2131 (3)	1586 (2)	2.31 (8)
O4(P2)	5708 (5)	2063 (3)	1524 (2)	2.20 (8)
O(W1)	4304 (5)	1846 (3)	−1627 (3)	2.64 (8)
O(W2)	1756 (5)	6577 (3)	−406 (3)	3.02 (9)
Co(2)[b]	0	0	0	1.41 (2)
O(W3)	1608 (5)	−28 (3)	1421 (2)	2.30 (7)
O(W4)	2614 (5)	−167 (3)	−795 (3)	2.95 (8)
O(W5)	728 (6)	−2033 (3)	954 (2)	3.09 (9)
Co(3)[b]	5000	0	5000	1.30 (2)
O(W6)	5994 (4)	−2096 (2)	5476 (2)	2.18 (7)
O(W7)	3032 (5)	−346 (3)	6270 (2)	2.49 (8)
O(W8)	7449 (5)	−398 (3)	6168 (2)	2.22 (7)
H1(N1)	515 (7)	557 (4)	757 (4)	1.7 (10)
H2(N1)	443 (8)	437 (5)	815 (4)	3.6 (13)
H3(N1)	571 (7)	440 (4)	719 (4)	1.5 (9)
H1(N2)	−64 (6)	550 (4)	769 (3)	1.3 (9)
H2(N2)	108 (7)	443 (4)	816 (3)	1.4 (9)
H3(N2)	−15 (8)	440 (5)	719 (4)	3.2 (12)
H1(N3)	86 (14)	712 (8)	716 (8)	10.6 (29)
H2(N3)	32 (17)	782 (10)	639 (9)	14.6 (39)
H3(N3)	259 (12)	750 (7)	669 (6)	7.7 (22)
H1(N4)	333 (7)	346 (4)	667 (4)	1.8 (10)
H2(N4)	399 (6)	417 (4)	560 (3)	1.0 (8)
H3(N4)	176 (8)	411 (4)	569 (4)	2.7 (11)
H(O1P2)	262 (9)	486 (5)	64 (5)	4.7 (15)
H1(W1)	427 (7)	210 (4)	−114 (4)	2.6 (11)
H2(W1)	568 (9)	133 (5)	−166 (5)	4.4 (15)
H1(W2)	248 (9)	688 (5)	−78 (5)	3.8 (13)
H2(W2)	40 (13)	707 (7)	−84 (7)	8.7 (24)
H1(W3)	128 (8)	−47 (4)	208 (4)	2.6 (11)
H2(W3)	163 (7)	72 (4)	135 (4)	1.7 (10)
H1(W4)	312 (8)	43 (5)	−101 (4)	3.2 (12)
H2(W4)	310 (9)	−83 (5)	−99 (5)	4.0 (14)
H1(W5)	102 (8)	−246 (5)	72 (4)	3.3 (12)
H2(W5)	110 (11)	−246 (7)	184 (6)	7.3 (21)
H1(W6)	703 (7)	−232 (4)	527 (4)	2.1 (10)
H2(W6)	520 (7)	−238 (4)	525 (4)	1.8 (10)
H1(W7)	209 (7)	22 (4)	622 (4)	1.6 (9)
H2(W7)	365 (9)	−72 (5)	690 (5)	4.6 (15)
H1(W8)	716 (8)	−72 (5)	675 (4)	3.3 (13)
H2(W8)	787 (7)	26 (4)	617 (4)	2.3 (11)

[a] Values are multiplied by 10^4 for nonhydrogen atoms and 10^3 for hydrogen atoms. [b] Co(2) and Co(3) have a multiplicity of 1/2. Only three of the water ligands around these atoms are given since the other three are found by inversion through the cobalt atom. [c] $B_{eq} = {}^4/_3\Sigma_i\Sigma_j\beta_{ij}a_ia_j$.

at 24 ppm assigned to $Co(NH_3)_4(PO_4)$, a broad singlet at 14 ppm assigned to $Co(NH_3)_4(H_2O)(HPO_4)$, and a singlet assigned to P_i. The ratio of complexed to free phosphate in solution was found to be 1:1 over a solution pH range of 2–8. The ratio of $Co(NH_3)_4(PO_4)$ to $Co(NH_3)_4(H_2O)(HPO_4)$ is a sensitive function of solution pH. The $Co(NH_3)_4(PO_4)$ to $Co(NH_3)_4(H_2O)(HPO_4)$ ratio measured at pH 4 was less than 0.05, at pH 5.5, 6.7, and 7.5 was 0.14, 0.64, and 2.9, respectively, and at pH 8.1 was more than 20. From these data the pK_a of $Co(NH_3)_4(H_2O)(HPO_4)$ was calculated to be ca. 7. The enthalpy of ionization was determined from the temperature dependence of the above ratio at pH 6.7 by using the van't Hoff equation. A ΔH ion of ca. +4 kcal/mol was calculated from the following ratios: 0.5 at 4 °C, 0.59 at 13 °C, 0.60 at 18 °C, 0.77 at 23 °C, and 0.8 at 28 °C.

Scheme I

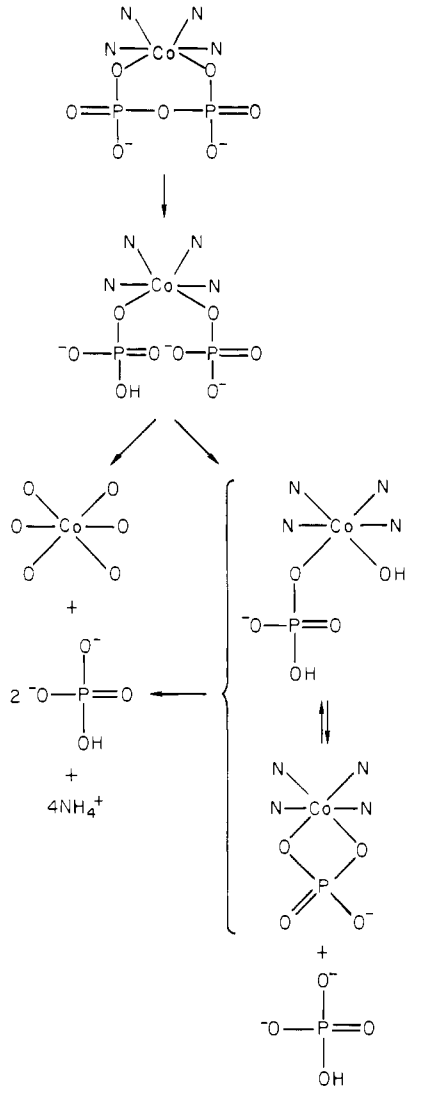

Discussion

Pyrophosphatase catalyzes the hydrolysis of P^1,P^2-bidentate $Co(NH_3)_4PP$ to cis, bis $Co(NH_3)_4(P_i)_2$ as the initial reaction product which is subsequently converted in solution to a mixture of monodentate $Co(NH_3)_4(H_2O)(HPO_4)$ and bidentate $Co(NH_3)_4(PO_4)$. The initial product could be released from the enzyme and be converted nonenzymatically into the observed mixture of final products, or alternatively, the initial reaction product could be converted to one of the final products on the enzyme active site as shown in Scheme II. In the case of the substitution-inert cobalt(III) complexes where the phosphate hydrolysis is very slow, pathway a predominates. The NMR studies show nearly complete conversion of substrate to the initial cis, bis $Co(NH_3)_4(P_i)_2$ product before any of the final products are observed; therefore, nearly all of the initial product must be released from the enzyme via pathway a. Although the enzyme does not appear to catalyze the conversion of the initial to the final reaction products (since the rate of this conversion is nearly equal with and without the enzyme), the enzyme active site may, however, provide a template for this conversion after the enzyme has completed

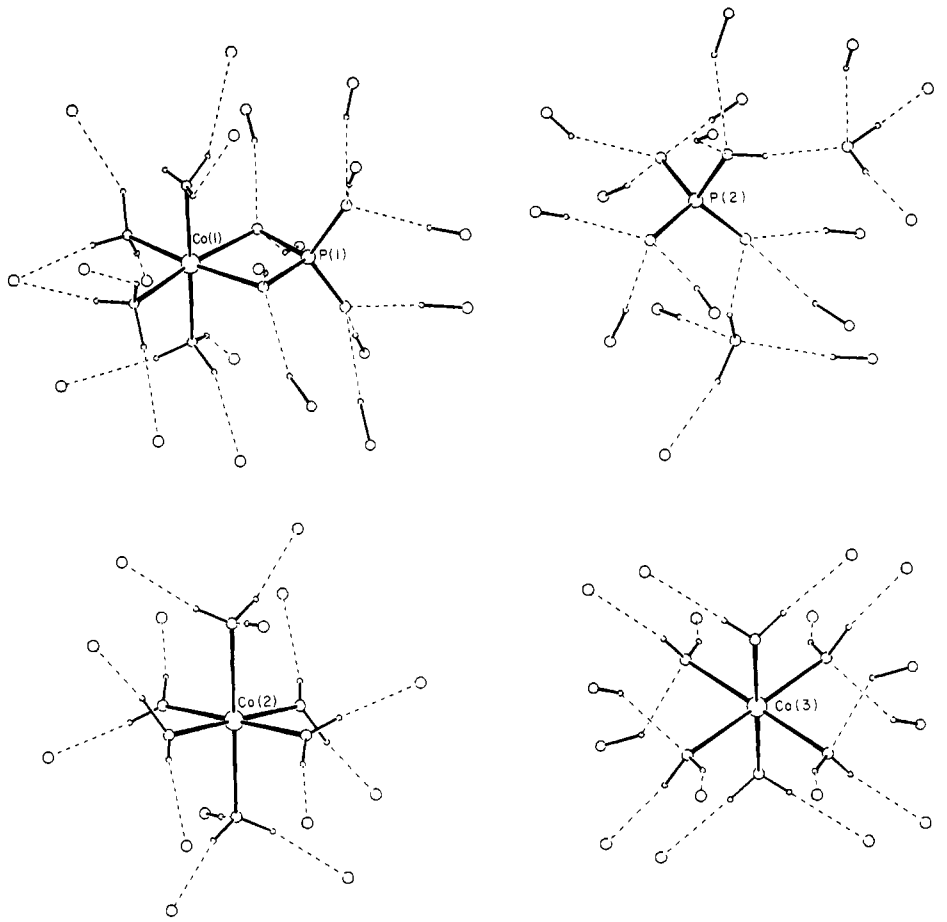

FIGURE 2: The hydrogen-bonding environment of the crystalline reaction product. Upper left, phosphato(cobalt) complex; upper right, orthophosphate and two water molecules; lower left, hexaaquocobalt(II) at (0, 0, 0); lower right, hexaaquocobalt(II) at ($^1/_2$, 0, $^1/_2$). Notice that every proton except H1(N3) is engaged in hydrogen bonding.

Table II: A List of All Hydrogen-Bonding Interactions Found in the Crystalline Reaction Product[a]

hydrogen bond A–H···B	symmetry code[a]	translation			distances (Å)			angle (deg)
		x	*y*	*z*	A–H	H···B	A···B	A–H···B
N(1)–H1(N1)···O1(P2)	2	1	1	1	0.98	2.21	3.056	161
N(1)–H2(N1)···O2(P2)	1	0	0	1	0.87	2.09	2.951	169
N(1)–H3(N1)···O3(P1)	2	1	1	1	0.95	2.09	3.041	172
N(2)–H1(N2)···O1(P2)	2	0	1	1	0.95	2.17	3.035	151
N(2)–H2(N2)···O2(P2)	1	0	0	1	0.82	2.11	2.920	167
N(2)–H3(N2)···O3(P1)	2	0	1	1	1.01	2.09	3.087	172
N(3)–H1(N3)					0.65			
N(3)–H2(N3)···O(W8)	1	−1	1	0	0.85	2.33	3.104	153
N(3)–H3(N3)···O(W7)	1	0	1	0	0.91	2.45	3.137	132
N(4)–H1(N4)···O(W1)	1	0	0	1	0.86	2.15	3.000	172
N(4)–H2(N4)···O2(P1)	2	1	1	1	0.94	2.07	2.950	157
N(4)–H3(N4)···O1(P1)	2	0	1	1	0.92	2.13	3.006	158
O1(P2)–H(O1P2)···O(W2)	1	0	0	0	0.82	1.81	2.622	169
O(W1)–H1(W1)···O2(P2)	1	0	0	0	0.79	2.00	2.744	158
O(W1)–H2(W1)···O(W3)	2	1	0	0	0.97	1.96	2.920	168
O(W2)–H1(W2)···O4(P2)	2	1	1	0	0.75	1.96	2.685	165
O(W2)–H2(W2)···O3(P2)	2	0	1	0	0.97	1.72	2.689	177
O(W3)–H1(W3)···O4(P1)	1	0	−1	0	0.85	1.89	2.730	170
O(W3)–H2(W3)···O3(P2)	1	0	0	0	0.85	1.89	2.714	165
O(W4)–H1(W4)···O(W1)	1	0	0	0	0.81	1.93	2.736	176
O(W4)–H2(W4)···O4(P2)	2	1	0	0	0.88	1.82	2.692	172
O(W5)–H1(W5)···O(W2)	1	0	−1	0	0.67	2.12	2.772	166
O(W5)–H2(W5)···O3(P1)	1	0	−1	0	1.02	1.67	2.678	172
O(W6)–H1(W6)···O1(P1)	1	1	−1	0	0.77	2.06	2.814	166
O(W6)–H2(W6)···O2(P1)	1	0	−1	0	0.82	1.97	2.783	168
O(W7)–H1(W7)···O4(P1)	2	0	1	1	0.76	2.01	2.748	163
O(W7)–H2(W7)···O4(P2)	2	1	0	1	0.79	1.91	2.645	154
O(W8)–H1(W8)···O3(P2)	2	1	0	1	0.72	2.03	2.674	149
O(W8)–H2(W8)···O4(P1)	2	1	1	1	0.90	1.83	2.711	167

[a] Symmetry codes: (1) *x*, *y*, *z* and (2) −*x*, −*y*, −*z*.

Scheme II

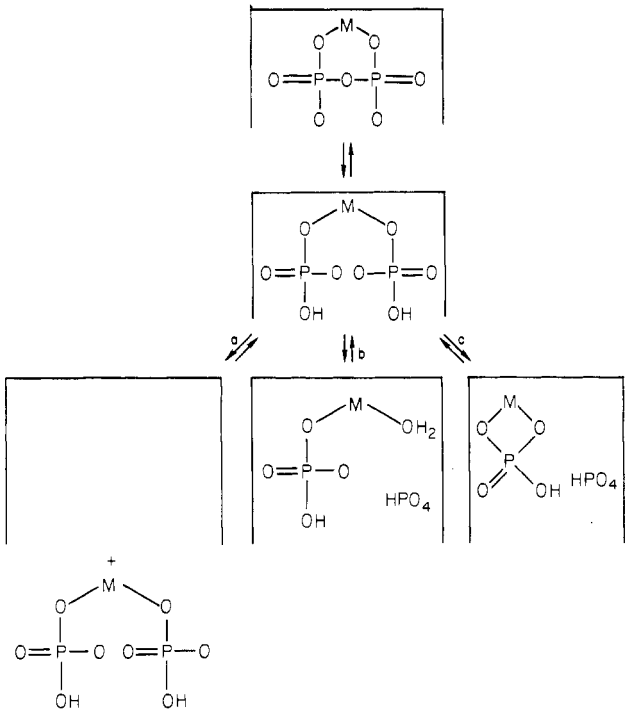

its primary task of converting substrate to initial product.

On the other hand, with divalent metal complexes such as MgPP or MnPP, where the coordination bonds undergo rapid ligand exchange, both phosphates are not constrained to leave simultaneously with the metal atom. In fact, Hamm & Cooperman (1978) demonstrated that in the presence of Mn^{2+} there are two unequivalent (one high affinity and one low affinity) phosphate bonding sites on the enzyme. Thus, for divalent metal ions, pathway a may be rejected since it requires that both phosphates bind with equal affinity.

This leaves the possibility of pathway b where the release of the first phosphate results in a monodentate metal–phosphate complex on the enzyme active site or pathway c which results in a bidentate metal–phosphate complex on the active site. The approach we took to distinguish between these paths was to first examine the structure and stability of $Co(NH_3)_4(PO_4)$. As indicated in Scheme II, pathways b and c may be distinguished on the basis of the form of MgP_i (monodentate or bidentate) which serves as the substrate in the reverse reaction. Thus, it is of interest to determine whether MgP_i in solution at physiological pH is monodentate or bidentate. The results from previous NMR studies (Tsai et al., 1980; Huang & Tsai, 1982) have suggested that when a six-membered chelate ring can be generated, polyphosphates will complex with Mg^{2+} to form bidentate complexes. Similarly, β,γ-bidentate Cr^{3+} and Co^{3+} complexes of ATP appear to be thermodynamically favored over the open γ-monodentate form as evidenced by the absence of detectable quantities of the latter. In solutions of bidentate ATP, complexes undergoing slow epimerization at the β-phosphate, via a γ-monodentate intermediate, do not significantly populate solutions of bidentate Cr(III)–ATP and Co(III)–ATP. The crystal structure of $Co(NH_3)_4(PO_4)$ (Figure 1) shows that unlike the six-membered chelate ring, the four-membered chelate ring is quite strained with the ring angles all considerably smaller than their ideal values. In fact, the ^{31}P NMR spectra of solutions prepared from the redissolved crystals reveal two different Co(III)–phosphate complexes, which suggests that in solution the bidentate complex undergoes ring opening. On the basis of absorption data, bidentate $Co(en)_2(PO_4)$ was found to

Scheme III

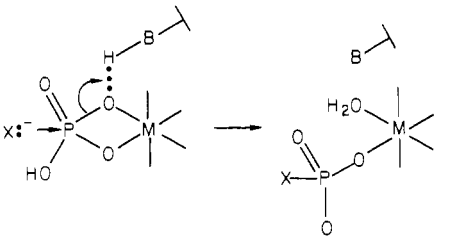

hydrolyze very slowly to monodentate $Co(en)_2(OH)(PO_4)$ ($t_{1/2}$ = 7.7 h) with the ratio of these two complexes at equilibrium being 33:1 (Lincoln & Stranks, 1968). In contrast, the $Co(en)_2(HPO_4)$ complex was reported to undergo rapid hydrolysis ($t_{1/2}$ = 2 min) to form monodentate $Co(en)_2(H_2O)(HPO_4)$ with an equilibrium ratio of 0.04:1. The ratio of these two species in solutions is thus determined by solution pH; by measuring this ratio as a function of pH we determined the pK_a of $Co(NH_3)_4(H_2O)(HPO_4)$ to be ca. 7 and the enthalpy of this ionization to be ca. +4 kcal/mol. These two values agree reasonably well with those measured by Lincoln & Stranks (1968) for the $Co(en)_2(H_2O)(HPO_4)$ complex.

The present results indicate that bidentate $Co(NH_3)_4P_i$ exists in solution only when the P_i ligand is fully deprotonated. The pK_a of $MgHPO_4$ as deduced from the reported stability constants (Smith & Martell, 1976) is 10.4, thus indicating that MgP_i will be protonated at physiological pH. If the bidentate isomer of $MgHPO_4$ is to exist in solution, the chelate ring strain associated with this complex must be significantly smaller than that of $Co(NH_3)_4(HPO_4)$. It is difficult in the absence of crystallographic data to predict the relative strain associated with the $MgHPO_4$ chelate ring, and therefore we must rely of pK_a data in order to assess the population of bidentate $MgHPO_4$ in solution. Accordingly, we predict that the pK_a of bidentate $MgHPO_4$ is ca. 7.6. This estimation is based on the pK_a of bidentate $Co(NH_3)_4(HPO_4)$ of 4.25 reported by Lincoln & Stranks (1968) and a 3.4 pK_a unit metal correction factor derived from the difference in pK_a of bidentate $Co(NH_3)_4PP$ (pK_a = 3) and MgPP [pK_a = 6.4 (Frey & Stuehr, 1972)]. The pK_a of monodentate $MgHPO_4$ is likely to be over 10 as the $-O-PO_3H$ ligand of Co(III) exhibits a pK_a of 8.5 (Lincoln & Stranks, 1968). Since the observed pK_a of $MgHPO_4$ is 10.4, it is reasonable to conclude that this complex is monodentate, not bidentate, in structure. Thus, if bidentate $MgHPO_4$ is a substrate for pyrophosphatase in the direction of pyrophosphate synthesis, it must be stabilized in the active site and therefore it is an activated form of orthophosphate. As indicated in Scheme III, this type of activation may be ideal for enzymes which catalyze condensation reactions between orthophosphate and nucleophiles.

In this manner the Mg^{2+} would activate the phosphorus atom via electron withdrawal, stabilize the departing hydroxide ion via coordination, and, by virtue of the chelate ring, provide a mechanism for strain catalysis (Farrell et al., 1969). This type of phosphate activation seems applicable to catalysis by the calcium–magnesium–ATPase of sarcoplasmic reticulum. This enzyme, as pointed out by Jencks (1980), has the remarkable ability to form an acyl phosphate spontaneously from inorganic phosphate. Pyrophosphatase, on the other hand, does not add P_i at the phosphoryl center of $MgHPO_4$ but rather at the metal center to generate the *cis*-$Mg(P_i)_2$ complex. Thus, stabilization of the bidentate $MgHPO_4$ complex in the active site would only serve to activate the Mg toward ligand exchange, a process which is clearly not needed. In addition, unlike pathway b, pathway c involving bidentate $MgHPO_4$

requires that the *cis*-$Mg(P_i)_2$ complex is an internal intermediate and as such it would not have direct access to solvent. Thus, the bis(phosphate) complex generated from an inert coordination complex of pyrophosphate should remain trapped in the active site of pyrophosphatase. This type of phenomenon is in fact observed with hexokinase-catalyzed reaction of glucose with bidentate CrATP wherein the bridged complex, $Cr(H_2O)_4$(glucose-6-P)(ADP), is trapped in the active site as a dead-end intermediate (Dunaway-Mariano & Cleland, 1980). As a result, one observes only single turnovers of CrATP by hexokinase. In contrast, the reaction rate of the pyrophosphatase-catalyzed hydrolysis of $Co(NH_3)_4PP$ as well as of $Cr(H_2O)_4PP$ (Knight et al., 1981) does not appear severely restricted by the rate of bis(phosphate) complex release, and therefore this complex must have access to the solvent. Therefore, pathway b of Scheme II appears to be most consistent with the data at hand. According to this pathway, the $Mg(H_2O)_4(P_i)_2$ is hydrolyzed directly to monodentate $Mg(H_2O)_5P_i$ which is subsequently released from the active site.

Supplementary Material Available

A table giving anisotropic thermal parameters for nonhydrogen atoms in the crystal structure, a list of all observed and calculated structure factors, and a stereo packing diagram of the crystal structure (13 pages). Ordering information is given on any current masthead page.

References

Anderson, B., Milburn, R. M., Harrowfield, J. M., Robertson, G. B., & Sargeson, A. M. (1977) *J. Am. Chem. Soc. 99*, 2652–2661.

Avaeva, S. M., Bakuleva, N. P., Baratwva, C. A., Nazarova, T. I., & Fink, N. Y. (1977) *Biochim. Biophys. Acta 482*, 173–184.

Cooperman, B. S., Panackal, A., Springs, B., & Hamm, D. J. (1981) *Biochemistry 20*, 6051–6060.

Cornelius, R. D., Hart, P. A., & Cleland, W. W. (1977) *Inorg. Chem. 16*, 2799–2805.

Cromer, D. T., & Waber, J. T. (1965) *Acta Crystallogr. 18*, 104–109.

Dunaway-Mariano, D., & Cleland, W. W. (1980) *Biochemistry 19*, 1506–1515.

Farrell, F. J., Kjellstrom, W., & Spiro, T. G. (1969) *Science (Washington, D.C.) 164*, 320–321.

Frey, C. M., & Stuehr, J. (1972) *J. Am. Chem. Soc. 94*, 8898–8904.

Hamm, D. J., & Cooperman, B. S. (1978) *Biochemistry 17*, 4033–4040.

Huang, S. L., & Tsai, M.-D. (1982) *Biochemistry 21*, 951–959.

International Tables for X-ray Crystallography (1974) Vol. IV, pp 148–151, Kynoch Press, Birmingham, England.

Jencks, W. P. (1980) *Adv. Enzymol. Relat. Areas Mol. Biol. 51*, 75–106.

Johnson, C. K. (1976) *ORTEP-II*, Report ORNL-5138, Oak Ridge National Laboratory, Oak Ridge, TN.

Knight, W. B., Fitts, S. W., & Dunaway-Mariano, D. (1981) *Biochemistry 20*, 4079–4086.

Konsowitz, D. M., & Cooperman, B. S. (1976) *J. Am. Chem. Soc. 98*, 1993–1995.

Lincoln, S. F., & Stranks, D. R. (1968) *Aust. J. Chem. 21*, 27–81.

Merritt, E. A., & Sundaralingam, M. (1980) *Acta Crystallogr., Sect. B B36*, 2576–2584.

Rapoport, T. A., Hohne, W. E., Heitman, P., & Rapoport, S. (1973) *Eur. J. Biochem. 33*, 341–347.

Smith, R. M., & Martell, A. E. (1976) *Critical Stability Constants*, Vol. 4, p 56, Plenum Press, New York.

Sperow, J. W., & Butler, L. G. (1976) *J. Biol. Chem. 251*, 2611–2612.

Springs, B., Welsh, K. M., & Cooperman, P. S. (1981) *Biochemistry 20*, 6384–6391.

Stewart, R. F., Davidson, E. R., & Simpson, W. T. (1965) *J. Chem. Phys. 42*, 3175–3187.

Tsai, M.-D., Huang, S. L., Kozlowski, J. J., & Chang, C. C. (1980) *Biochemistry 19*, 3531–3536.

Three-Dimensional Structure of the Complex of the *Rhizopus chinensis* Carboxyl Proteinase and Pepstatin at 2.5-Å Resolution†

R. Bott,* E. Subramanian, and D. R. Davies

ABSTRACT: An X-ray diffraction analysis has been carried out at 2.5-Å resolution of the three-dimensional structure of the *Rhizopus chinensis* carboxyl proteinase complexed with pepstatin. The resulting model of the complex supports the hypothesis [Marciniszyn, J., Hartsuck, J. A., & Tang, J. (1976) *J. Biol. Chem. 251*, 7088–7094] that statine (3-hydroxy-4-amino-6-methylheptanoic acid) approaches an analogue of the transition state for catalysis. The way in which pepstatin binds to the enzyme can be extended to provide a model of substrate binding and a model of the transition-state complex. This in turn has led to a proposed mechanism of action based on general acid–base catalysis with no covalent intermediates. These predictions are in general agreement with kinetic studies using several carboxyl proteinases, which together with their sequence homology and their common three-dimensional structures suggest that this mechanism can be extrapolated to all carboxyl proteinases.

No consensus exists on the mechanism of action of the carboxyl proteinases, despite the fact that they have been widely studied (Fruton, 1976; Tang, 1979; James, 1981; Clement, 1973; Silver & James, 1980; Antonov, 1978). This class of proteinase includes the mammalian enzymes pepsin, chymosin, renin, and cathepsin D, as well as a variety of fungal enzymes. All the carboxyl proteinases hitherto examined appear to be highly conserved in that they all have two active

† From the Laboratory of Molecular Biology, National Institute of Arthritis, Diabetes, and Digestive and Kidney Diseases, National Institutes of Health, Bethesda, Maryland 20205. *Received July 20, 1982.*